JACS
JOURNAL OF THE AMERICAN CHEMICAL SOCIETY
Communication
pubs.acs.org/JACS

Hybrid Solar Cells with Outstanding Short-Circuit Currents Based on a Room Temperature Soft-Chemical Strategy: The Case of P3HT:Ag_2S

Yan Lei,[†,‡] Huimin Jia,[†] Weiwei He,[†] Yange Zhang,[†] Liwei Mi,[†] Hongwei Hou,[‡] Guangshan Zhu,[†,§] and Zhi Zheng*[,†]

[†]Key Laboratory of Micro-Nano Materials for Energy Storage and Conversion of Henan Province and Institute of Surface Micro and Nano Materials, Xuchang University, Henan 461000, China

[‡]Department of Chemistry, Zhengzhou University, Zhengzhou 450000, China

[§]State Key Laboratory of Inorganic Synthesis and Preparative Chemistry, Jilin University, Changchun 130012, China

Supporting Information

ABSTRACT: P3HT:Ag_2S hybrid solar cells with broad absorption from the UV to NIR band were directly fabricated on ITO glass by using a room temperature, low energy consumption, and low-cost soft-chemical strategy. The resulting Ag_2S nanosheet arrays facilitate the construction of a perfect percolation structure with organic P3HT to form ordered bulk heterojunctions (BHJ); without interface modification, the assembled P3HT:Ag_2S device exhibits outstanding short-circuit current densities (J_{sc}) around 20 mA cm^{-2}. At the current stage, the optimized device exhibited a power conversion efficiency of 2.04%.

With the rapid and productive development of nanoscience and nanotechnology, research focused toward developing various materials of nanoscale are not limited to creating novel nanostructures.[1] The development of a designed low-cost and low energy-consumption approach to easily construct desirable nanostructures becomes increasingly important due to the practical industrial applications in the near future. For example, in the design and fabrication of solar cell materials and devices, scientists have noted that most of the common physical and chemical processes inevitably consume considerable energy prior to the energy generation from final devices.[2] On the other hand, the use of toxic compounds, such as Cd and Pb, will be eventually terminated due to the increasingly stringent environmental requirement. As Grätzel[3] pointed out, chemistry is expected to make important contributions to identify environmentally friendly solutions to energy and environmental problems. Seeking new strategies for low cost and low energy consumption to invent low toxic solar cell materials is not only academically important but also industrially demanding.

Solution-processed photovoltaic devices, such as the inorganic−organic hybrid thin film solar cell devices, are promising candidates because they may offer an opportunity to harvest solar energy in a simplified, low cost, and mechanically flexible way. In 2002, Alivisatos reported the fabrication of P3HT:CdSe hybrid thin film solar cells as groundbreaking with an ∼1.7% conversion efficiency by using the solution processed route.[4] In the past 10 years, many chemists have been devoted to developing new materials and strategies for potential industrial application of such solution-processed approaches.[5] Compared with the dye-sensitized and pure conjugated polymer solar cells, the hybrid thin film solar cells based on conjugated polymer/inorganic nanocrystals have several advantages and thus gained much attention in the field of synthetic chemistry.[6] However, this type of hybrid solar cells is still not ideal for future industrial and commercial applications because of the relatively high reaction temperature which is necessary for synthesizing the chacolgenide nanocrystals,[7] the undesirable insulators of surfactants, self-assembled monolayer or long chain ligands capped on the as-synthesized NCs, and loose contact of the active layer on the electrodes.

In our previous studies, we have successfully developed a facile solvothermal approach for fabricating hybrid thin film solar cell devices,[8] which have partially solved the above-mentioned deficiencies although the efficiency was not high. Aiming at further decreasing the energy consumption and improving the photovoltaic performance, here, we demonstrate a simplified, room temperature processing, large scale, solvent recycling, and low-cost strategy for *in situ* fabrication of Ag_2S nanosheet-like arrays and P3HT:Ag_2S hybrid films directly on ITO glass for thin film solar cell devices. We selected Ag_2S, as it is a near-infrared absorbed binary semiconductor with a narrow band gap of ∼0.9 eV,[9] and it is environmentally friendly and stable enough to acid, base, and moisture. This is the first report using Ag_2S as the electron acceptor and main absorbing layer in hybrid thin film solar cells. The current strategy possesses the following advantages: First, all of the material fabrication and device assembly processes were performed at room temperature and thus consumed negligible energy; Second, the resulting Ag_2S nanosheet arrays facilitated the construction of a perfect percolation structure with organic P3HT to form an ordered hybrid bulk heterojunction (BHJ); Third, the assembled P3HT:Ag_2S devices utilized a broader solar spectrum from the UV to NIR region and exhibited outstanding short-circuit current densities (J_{sc}) around 20 mA cm^{-2} without interface modification. To our knowledge, this is the highest J_{sc} value among the reported organic−inorganic hybrid solar cells; Fourth, the *in situ* fabricated devices on ITO

Received: July 31, 2012
Published: October 8, 2012

   dx.doi.org/10.1021/ja307521t | J. Am. Chem. Soc. 2012, 134, 17392−17395

are both chemically and mechanically stable for potential industrial applications.

In the present reaction design, an elemental silver layer was first prepared on the ITO glass substrate. In a typical procedure, the elemental silver coated ITO glass and 0.01 g sulfur powders were put into a 20 mL vessel, and then 15 mL of *N*,*N*-dimethylformamide (DMF) was added. The container was maintained at 25 °C for 8 h. Finally, a black thin film on the ITO substrate was obtained, and the solvent can be saved for later use. The X-ray diffraction (XRD) pattern demonstrated the formation of pure Ag_2S thin film (Figure S2, JCPDS File No. 14-72, monoclinic).

The transformation process from the initial elemental Ag layer to the Ag_2S and P3HT:Ag_2S composite thin film was described in Figure 1. The original magnetron sputtered Ag

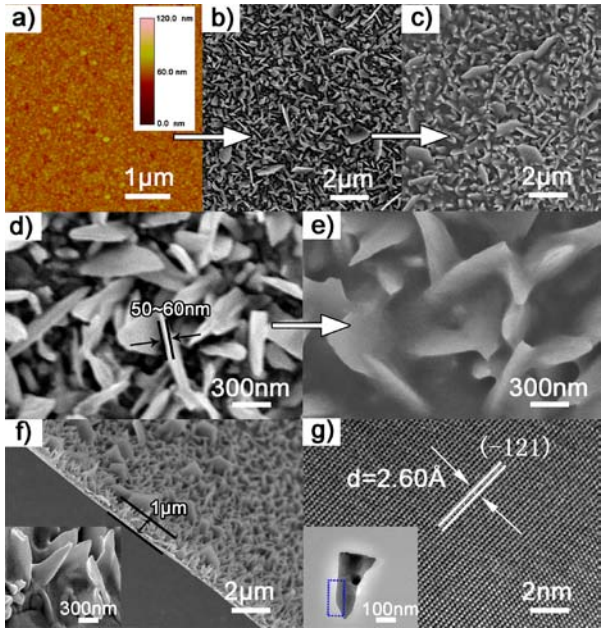

Figure 1. (a) AFM image of the nanosized elemental Ag surface; (b) low-magnification SEM image of the as-prepared Ag_2S nanosheet film; (c) low-magnification SEM image of P3HT:Ag_2S hybrid thin film; (d) magnified SEM image of Ag_2S nanosheet film; (e) magnified SEM image of P3HT:Ag_2S hybrid thin film; (f) cross section SEM image of the P3HT:Ag_2S hybrid thin film; (g) HRTEM images of Ag_2S nanosheet (the dotted line frame in the inserted image illustrates the selected area of an individual Ag_2S nanosheet).

surface was assembled by nanosized elemental silver grains (about 60−80 nm in diameter, as shown in Figure 1a). After 8 h of reaction with elemental sulfur at 25 °C, all of the silver patterned area is covered with nanosheet Ag_2S instead, indicating that particular elemental silver film was completely transformed into ordered Ag_2S nanosheet arrays (Figure 1b). In the fabrication of hybrid solar cell devices, this step is important because it directly formed an ordered and stable inorganic template which is rooted in the ITO electrode, without consumption of energy. The SEM image of the as-formed P3HT:Ag_2S hybrid film (Figure 1c) demonstrates that the ordered Ag_2S (n-type) nanosheet array surface was uniformly covered with conjugated P3HT (p-type) after infiltrating. This construction process was further clearly displayed by magnifying Figure 1b and c, respectively. We can see a good deal of interstices between the nanosheet arrays, and the thickness of an individual Ag_2S nanosheet was about 50−60 nm (Figure 1d).

A P3HT-chloroform solution was first selected and spin-coated on the above ordered and stable Ag_2S/ITO template to form an active layer. As we designed, all surfaces of the nanosheet arrays and those interstices were effectively infiltrated and covered by organic P3HT to form an ordered hybrid thin film (Figure 1e) and thus ensuring a large surface area for charge separation. From the cross section SEM image (Figure 1f), the active layer thickness of the whole P3HT:Ag_2S hybrid thin film was measured to be about 1 μm. There is still a compact Ag_2S semiconductor layer between the Ag_2S nanosheet arrays and the ITO substrate, which can effectively avoid the internal short circuit in the solar cell devices. The inset image shows distinctly that all Ag_2S nanosheet surfaces were surrounded by organic P3HT. This specific domain contains built-in percolation pathways for effective electron or hole transport. Figure 1g shows the TEM and HRTEM of the Ag_2S nanosheet, the well-resolved 2D lattice fringes with a lattice spacing of 2.60 Å correspond to the (−121) plane of the monoclinic Ag_2S. Thus, we further demonstrated that the room-temperature fabricated Ag_2S film could also be well crystallized. Overall, the fabricated ripple structures of the organic−inorganic hybrid layer may provide a large interfacial surface area with a large number of heterojunctions and reduce the loss of sunlight intensity for efficient light harvesting.

To fabricate the organic−inorganic hybrid solar cell devices, Au was then thermally evaporated on the P3HT:Ag_2S active layer as the anode. The configuration and each component energy band of the completed hybrid solar cell device were shown in Figure 2a and 2b, respectively. We can clearly see that

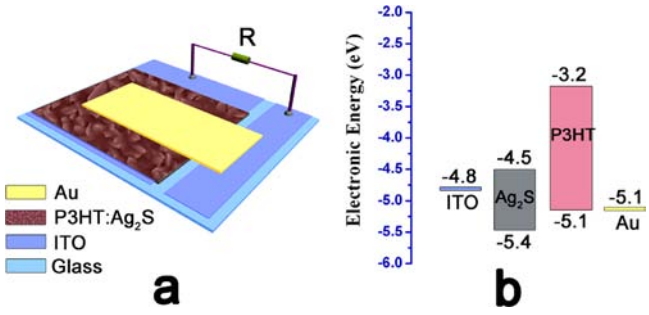

Figure 2. (a) Schematic device structure of the designed ITO/Ag_2S:P3HT/Au hybrid solar cells; (b) corresponding energy levels of the assembled hybrid thin film photovoltaic device.

the HOMO (−3.2 eV) and LUMO (−5.1 eV) levels of conjugated P3HT are well above the conduction band bottom (−4.5 eV) and valence band top (−5.4 eV) of Ag_2S. In our current device, the possible mechanism of photoelectric conversion may involve the incident photons being adsorbed by the P3HT:Ag_2S active layer and the generated excitons becoming well separated on the interfaces of Ag_2S and P3HT. After the exciton dissociation, electrons are injected into the conduction band of Ag_2S and further to the ITO cathode, while the holes travel to the HOMO of P3HT and the Au anode.

The photovoltaic performance of such a Au/P3HT:Ag_2S/ITO device with an active area of 0.15 cm^2 was investigated at room temperature in air under simulated AM1.5 solar irradiation (100 mW cm^{-2}), and the illumination of light was precisely calibrated by a standard silicon solar cell. The performance of the original device exhibited an open-circuit

dx.doi.org/10.1021/ja307521t | J. Am. Chem. Soc. 2012, 134, 17392−17395

voltage (V_{oc}) of 0.18 V, a short-circuit current density (J_{sc}) of 9.90 mA cm^{-2}, a fill factor (FF) of 27.82%, and a conversion efficiency (η) of 0.50%, which was prepared by using chloroform as solvent for P3HT casting. Although this result revealed a low open-circuit voltage and fill factor, it is interesting to note that, after a simple drying treatment in a glovebox at room temperature for 24 h, the performance of the hybrid thin film device was significantly improved. Figure 3a

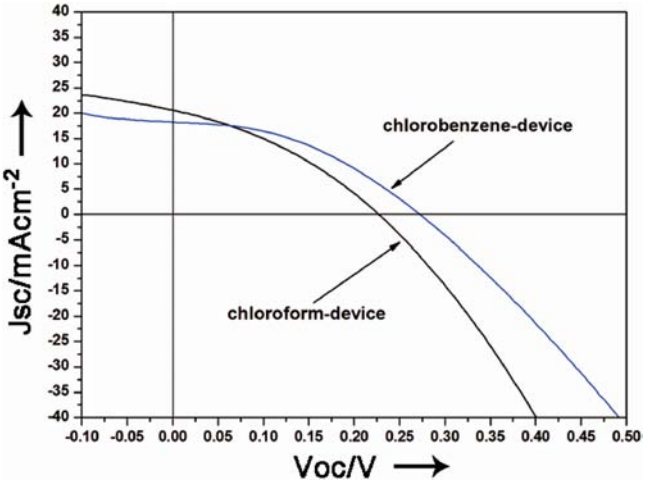

Figure 3. $J-V$ characteristics of the chlorobenzene-P3HT:Ag_2S and chloroform-P3HT:Ag_2S hybrid thin film solar cells.

plots the characteristics of such an improved device, which exhibits a V_{oc} of 0.22 V, a J_{sc} of as high as 20.55 mA cm^{-2}, an FF of 38.41%, and an η of 1.61%. We attribute this meaningful phenomenon to increases in the carrier mobility and degree of organization of P3HT during the slow drying process,[10] which is consistent with Olson's study[11] in the fabrication of the ZnO based hybrid solar cell device. The photovoltaic performance of the P3HT:Ag_2S devices did not weaken compared with the initial devices even after 8 months of storage in a general desiccator without encapsulation (see Supporting Information for video file).

Considering that the solvent with a high boiling point may lead to a higher degree of organization and better infiltration of P3HT into the ordered Ag_2S array,[12] we recently investigated the solar cell performance using chlorobenzene as solvent for P3HT casting. The curve of such a chlorobenzene device (Figure 3a) demonstrates an increased V_{oc} of 0.27 V, a J_{sc} of 18.20 mA cm^{-2}, an FF of 45.90%, and an η of 2.04%. Such behaviors indicate that the interaction between P3HT molecules in the thin film plays an important role in improving the performance of hybrid solar cells. Control experiments demonstrated that the current 10 mg/mL is a proper level of concentration of P3HT for constructing an effective P3HT:Ag_2S percolation structure. The dark current was also measured under the same conditions without illumination (Figure S4), revealing that the dark current of the chlorobenzene device compared to the chloroform device was lower, so that the chlorobenzene device brought out a higher open voltage.[13]

The external quantum efficiency (EQE) data of P3HT:Ag_2S hybrid solar cell are shown in Figure 4a. Interestingly, the hybridization of P3HT with an ordered Ag_2S nanosheet has led to a significant improvement of EQE from the UV–vis to near-IR region. The maximum EQE is about 45% at 675 nm, and the

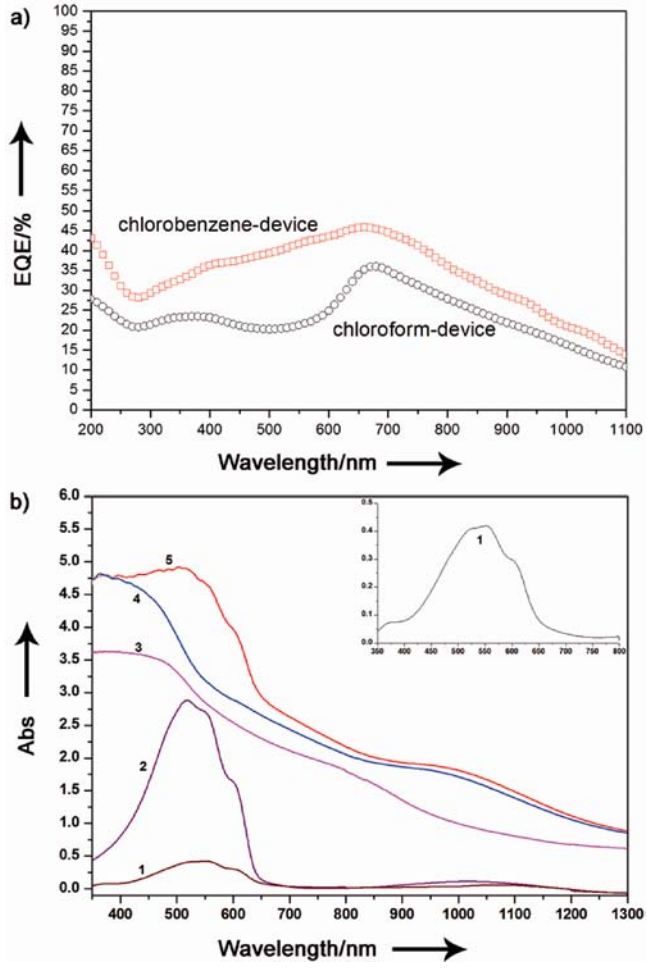

Figure 4. (a) EQE data of ITO/Ag_2S:P3HT/Au hybrid solar cells; (b) UV–vis–NIR spectra of (1) pristine chlorobenzene-P3HT thin film; (2) chloroform-P3HT thin film; (3) Ag_2S thin film; (4) chlorobenzene-P3HT:Ag_2S; and (5) chloroform-P3HT:Ag_2S hybrid thin films. The inserted curve reveals the detail of the chloroform-P3HT thin film.

EQE value can still reach 15% at 1100 nm (data beyond 1100 nm were not collected). It is also interesting to note that even the solar spectrum between 1100 and 2350 nm could still be absorbed by the Ag_2S nanosheet film (Figure S6). However, the generally prepared conjugated polymer/inorganic crystal hybrid film could only utilize the light from 300 to 700 nm. The current extremely broad spectra of EQE responds to the improved absorption of the P3HT:Ag_2S hybrid thin film. Figure 4b shows the UV–vis–NIR spectra of pristine chlorobenzene-P3HT (Figure 4b$_1$), chloroform-P3HT (Figure 4b$_2$), Ag_2S films (Figure 4b$_3$), chlorobenzene-P3HT:Ag_2S (Figure 4b$_4$), and chloroform-P3HT:Ag_2S (Figure 4b$_5$) hybrid films. An onset at ~620 nm, a shoulder at ~550 nm, and a peak at ~520 nm were absorption features of the pristine P3HT solid film (Figure 4b$_1$ and 4b$_2$). The intensity of Figure 4b$_1$ compared to Figure 4b$_2$ was significantly weaker because the P3HT layer spin-casted from chloroform was thicker than that from chlorobenzene under the same conditions. The persistent wide absorption property of the Ag_2S thin film from the ultraviolet to near-IR region was recorded in Figure 4b$_3$. We can clearly see that the absorption spectra of the chloroform-P3HT:Ag_2S hybrid film (Figure 4b$_5$) exhibited features of both pristine P3HT and the Ag_2S nanocrystal thin film, while the chlorobenzene-

dx.doi.org/10.1021/ja307521t | J. Am. Chem. Soc. 2012, 134, 17392–17395

P3HT:Ag_2S hybrid film (Figure 4b$_4$) mainly exhibited the absorbance of Ag_2S nanocrystals due to less P3HT coating. Therefore, in the current hybrid thin film prepared from chlorobenzene, light is predominately absorbed in the Ag_2S layer.

The EQE data show that only the photons with energies greater than 1.9 eV can be used for photovoltaic conversion in traditional P3HT and nanocrystal particle hybrid solar cells,[14] which means that light is predominately absorbed in P3HT and the highest J_{sc} is only ~14 mA cm^{-2} in theory. However, Ag_2S with a band gap of 0.9 eV will lead to a theoretical J_{sc} as high as ~51 mA cm^{-2}.[15] In our device the J_{sc} can be more than 20 mA cm^{-2}. Based on these collected data, we believe that the Ag_2S ripple layer as the ordered template is the predominant absorber in the P3HT:Ag_2S hybrid solar cells and thus induced the unusually high J_{sc}. The photovoltaic performances could be further improved with parameter optimization.

In summary, we demonstrate a simplified, large scale, solvent recycling, and low-cost soft chemical strategy to *in situ* fabricate Ag_2S nanosheet-like arrays and P3HT:Ag_2S hybrid films directly on ITO glass for thin film solar cell devices. All of the material fabrication and device assembly processes were performed at room temperature and thus consumed negligible energy. The resulting Ag_2S nanosheet arrays facilitate the construction of a perfect percolation structure with organic P3HT to form an ordered hybrid bulk heterojunction (BHJ). More importantly, without interface modification, the assembled P3HT:Ag_2S devices exhibited outstanding short-circuit current densities (J_{sc}) around 20 mA cm^{-2}. At the current stage, the optimized device exhibited a power conversion efficiency of 2.04%. Based on the EQE and UV–vis analysis, we believe that the Ag_2S ripple layer is the predominant absorber in the current P3HT:Ag_2S hybrid solar cells and the photovoltaic performances could be further enhanced with device optimization. Further investigation is in progress to decrease the dark-current density toward a higher open-circuit voltage value. This simple strategy is also expected to fabricate other I–VI group based hybrid solar cell materials.

■ ASSOCIATED CONTENT

Ⓢ Supporting Information

Experimental details, growth process of Ag_2S thin film, XRD pattern of Ag_2S thin film on ITO substrate, photos of P3HT:Ag_2S device fabrication, and the dark current data of the device. This material is available free of charge via the Internet at http://pubs.acs.org.

■ AUTHOR INFORMATION

Corresponding Author

zhengzhi99999@gmail.com

Notes

The authors declare no competing financial interest.

■ ACKNOWLEDGMENTS

This work was supported by the National Natural Science Foundation of China (Grant Nos. 21273192, 20873118, 91023010, 11004168), Program for New Century Excellent Talents in University (Grant NCET-08-0665), the Program for Science & Technology Innovation Talents in Universities of Henan Province (2008 HASTIT016), and Innovation Scientists and Technicians Troop Construction Projects of Henan Province (Grant No. 104100510001).

■ REFERENCES

(1) (a) Wang, Z. L. *Adv. Mater.* **2012**, *24*, 280–285. (b) Bakke, J. R.; Pickrahn, K. L.; Brennan, T. P.; Bent, S. F. *Nanoscale* **2011**, *3*, 3482–3508. (c) Fan, Z. Y.; Razavi, H.; Do, J. W.; Moriwaki, A.; Ergen, O.; Chueh, Y. L.; Leu, P. W.; Ho, J. C.; Takahashi, T.; Reichertz, L. A.; Neale, S.; Yu, K.; Wu, M.; Ager, J. W.; Javey, A. *Nat. Mater.* **2009**, *8*, 648–653.

(2) Meng, T. *Electrochem. Soc. Interface* **2008**, *17*, 30–35.

(3) Gratzel, M. *Inorg. Chem.* **2005**, *4*, 6841–6851.

(4) Huynh, W. U.; Dittmer, J. J.; Alivisatos, A. P. *Science* **2002**, *295*, 2425–2427.

(5) Reiss, P.; Couderc, E.; Girolamo, J. D.; Pron, A. *Nanoscale* **2011**, *3*, 446–489.

(6) (a) Liu, C. Y.; Holman, Z. C.; Kortshagen, U. R. *Nano Lett.* **2009**, *9*, 449–452. (b) Weickert, J.; Dunbar, R. B.; Hesse, H. C.; Wiedemann, W.; Schmidt-Mende, L. *Adv. Mater.* **2011**, *23*, 1810–1828. (c) Chang, J. A.; Rhee, J. H.; Im, S. H.; Lee, Y. H.; Kim, H. J.; Seok, S. I.; Nazeeruddin, M. K.; Gratzel, M. *Nano Lett.* **2010**, *10*, 2609–2612.

(7) Todorov, T. K.; Reuter, K. B.; Mitzi, D. B. *Adv. Mater.* **2010**, *22*, E156–E159.

(8) (a) Jia, H. M.; He, W. W.; Chen, X. W.; Lei, Y.; Zheng, Z. *J. Mater. Chem.* **2011**, *21*, 12824–12828. (b) Li, D. P.; Zheng, Z.; Lei, Y.; Yang, F. L.; Ge, S. X.; Zhang, Y. D.; Huang, B. J.; Gao, Y. H.; Wong, K. W.; Lau, W. M. *Chem.—Eur. J.* **2011**, *17*, 7694–7700. (c) Li, D. P.; Zheng, Z.; Lei, Y.; Ge, S. X.; Zhang, Y. D.; Zhang, Y. G.; Wong, K. W.; Yang, F. L.; Lau, W. M. *CrystEngComm* **2010**, *12*, 1856–1861.

(9) Xu, Y.; Schoonen, M. A. A. *Am. Mineral.* **2000**, *85*, 543–556.

(10) (a) Li, G.; Shrotriya, V.; Huang, J. S.; Yao, Y.; Moriarty, T.; Emery, K.; Yang, Y. *Nat. Mater.* **2005**, *4*, 864–868. (b) Li, G.; Yao, Y.; Yang, H.; Shrotriya, V.; Yang, G. W.; Yang, Y. *Adv. Funct. Mater.* **2007**, *17*, 1636–1644. (c) Mihailetchi, V. D.; Xie, H. X.; Boer, B. D.; Popescu, L. M.; Hummelen, J. C. *Appl. Phys. Lett.* **2006**, *89*, 012107.

(11) Olson, D. C.; Lee, Y. J.; White, M. S.; Kopidakis, N.; Shaheen, S. E.; Ginley, D. S.; Voigt, J. A.; Hsu, J. W. P. *J. Phys. Chem. C* **2007**, *111*, 16640–16645.

(12) Dang, M. T.; Wantz, G.; Bejbouji, H.; Urien, M.; Dautel, O. J.; Vignau, L.; Hirsch, L. *Sol. Energy Mater. Sol. Cells* **2011**, *95*, 3408–3418.

(13) Avasthi, S.; Lee, S.; Loo, Y. L.; Sturm, J. C. *Adv. Mater.* **2011**, *23*, 5762–5766.

(14) (a) Zhang, W.; Zhu, R.; Li, F.; Wang, Q.; Liu, B. *J. Phys. Chem. C* **2011**, *115*, 7038–7043. (b) Gur, I.; Fromer, N. A.; Chen, C. P.; Kanaras, A. G.; Alivisatos, A. P. *Nano Lett.* **2007**, *7*, 409–414. (c) Liu, C. Y.; Holman, Z. C.; Kortshagen, U. R. *Nano Lett.* **2009**, *9*, 449–452. (d) Kim, S. J.; Kim, W. J.; Cartwright, A. N.; Prasad, P. N. *Appl. Phys. Lett.* **2008**, *92*, 191107. (e) Spoerke, E. D.; Lloyd, M. T.; McCready, E. M.; Olson, D. C.; Lee, Y. J.; Hsu, J. W. P. *Appl. Phys. Lett.* **2009**, *95*, 213506.

(15) Dennler, G.; Scharber, M. C.; Brabec, C. J. *Adv. Mater.* **2009**, *21*, 1323–1338.